


**Please cite the Published Version**

Khan, Thawhid, Taufiqurrakhman, Mohamad, Merrell, Charlotte, Pryce, Greg, Danturthi, Atreya, Liskiewicz, Tomasz , Pandit, Hemant, Yan, Yu and Bryant, Mike (2025) Enhancing fretting performance of 316L biomedical alloys through duplex TiN and DLC coatings. Surface Innovations. pp. 1-29. ISSN 2050-6252

**DOI:** <https://doi.org/10.1680/jsuin.24.00099>

**Publisher:** Emerald

**Version:** Accepted Version

**Downloaded from:** <https://e-space.mmu.ac.uk/638315/>

**Usage rights:**  [Creative Commons: Attribution 4.0](https://creativecommons.org/licenses/by/4.0/)

**Additional Information:** This is an author-produced version of the published paper. Uploaded in accordance with the University's Research Publications Policy.

**Data Access Statement:** Data will be made available on request.

**Enquiries:**

If you have questions about this document, contact [openresearch@mmu.ac.uk](mailto:openresearch@mmu.ac.uk). Please include the URL of the record in e-space. If you believe that your, or a third party's rights have been compromised through this document please see our Take Down policy (available from <https://www.mmu.ac.uk/library/using-the-library/policies-and-guidelines>)

# Enhancing fretting performance of 316L biomedical alloys through duplex TiN and DLC coatings

Thawhid Khan<sup>1</sup>, Mohamad Taufiqurrakhman<sup>2</sup>, Charlotte Merrell<sup>2</sup>, Greg Pryce<sup>2</sup>, Atreya Danturthi<sup>2</sup>, Tomasz Liskiewicz<sup>3</sup>, Hemant Pandit<sup>4</sup>, Yu Yan<sup>5</sup> and Mike Bryant<sup>6</sup>

<sup>1</sup>Department of Mechanical Engineering, University of Sheffield, Mappin Street, Sheffield, S1 3JD, UK

<sup>2</sup>Institute of Functional Surfaces, University of Leeds, School of Mechanical Engineering, Leeds, LS2 9JT, UK

<sup>3</sup>Faculty of Science and Engineering, Manchester Metropolitan University, Chester Street, Manchester M15 6BH, UK

<sup>4</sup>Leeds Institute of Rheumatic and Musculoskeletal Medicine (LIRMM), University of Leeds, Chapel Allerton Hospital, Leeds LS7 4SA, UK

<sup>5</sup>Corrosion and Protection Center, Institute for Advanced Materials and Technology, University of Science and Technology Beijing, Beijing 100083, China

<sup>6</sup>University of Birmingham, School of Mechanical Engineering, Haworth Building, Edgbaston, B15 2GR, West Midlands, UK

\*Corresponding author: Thawhid Khan (thawhidkhan@yahoo.co.uk)

**Keywords:** Duplex coatings, TiN, DLC, fretting, nitriding

## Abstract

This study investigates the use of duplex coatings, TiN/DLC, on improving the tribological performance of stainless steel 316L which is commonly used for femoral stems in total hip replacement implants. A range of substrate pre-treatment variants (nitriding and polishing) were applied to investigate the impact on the mechanical and tribological performance of the coatings. The tribological performance of plasma Vapour Deposition (PVD) duplex coating variants were tested using a bespoke in-house fretting tribometer with an electrodynamic shaker utilising a ball-on-plate configuration. Fretting was replicated by applying micro-motion to the Ø12 Al<sub>2</sub>O<sub>3</sub> ball relative to duplex coated SS 316L plates under a dead weight normal load. Un-polished substrates prior to the coating deposition led to improved tribological performance likely due to improve coating adhesion to the substrate surface. The hydrogenated DLC sample variants showed lower friction performance compared to hydrogen-free DLC variants most likely due to higher amounts of graphitisation.

## 1. Introduction

Total hip replacement (THR) is commonly used to treat end-stage hip osteoarthritis, even with increased implant lifetimes and procedure success rates, there are still some implant failures. Implant retrieval studies have shown that fretting-corrosion at the interface between modular components such as the head-neck taper junction due to relative micromotions and the corrosive environment, is one of the key causes for implant failure<sup>1-9</sup>.

In India and China, there is an uptake in the wide use of austenitic stainless-steel (SS) 316L in orthopaedic implants specifically for femoral stems. This is due to their cost effectiveness, wide availability and ease of manufacturing compared to Ti and Co-based alloys. AISI 316L SS is the primary recommended grade for implant applications, where the presence of chromium activates a thin and passive oxide layer that helps to protect the surface against corrosion<sup>10</sup>. The mechanical properties such as fracture toughness and tribological performance can be modified with an increase in carbon content. Their load-bearing capacity makes them an ideal material candidate for orthopaedic implants<sup>11</sup>.

1 However, the failure of these SS implants in-vivo due to tribocorrosion, which is where the interface of  
2 the metallic components at the taper junction experiences wear and corrosion <sup>12</sup>, leading to the release  
3 of toxic metal ion such as nickel and chromium into the body causing allergic reactions <sup>13</sup>.

4 To improve the durability and bio-integration of implants two approaches can be taken. The first  
5 involves the deposition of organic or inorganic-based coatings on to the metallic surface without  
6 modifying the properties of the substrate. The second approach uses conversion coatings or surface  
7 modified layers, where the thickness is increased by the chemical modification of the substrate. Surface  
8 preparation for both methods by grinding or polishing can influence surface roughness to improve the  
9 mechanical interlocking of the coatings <sup>13-16</sup>. This study utilises the deposition of two different coatings  
10 using the Physical Vapour Deposition (PVD) technique <sup>17</sup>.

11 Nitride coatings such as TiN have been proposed as protective coatings for the orthopaedic implants to  
12 protect against wear and tear and to act as diffusion barrier layer preventing the ion release from the SS  
13 316L substrate into the human body. TiN coatings are shown to have excellent chemical stability,  
14 biocompatibility and hardness making them a potential candidate to be used in arthroplasty. However  
15 due to the micro-cracks, pores and transient grain boundaries, in certain applications these coatings can  
16 exhibit poor wear and corrosion resistance during <sup>18</sup>. The dissimilarity in elastic modulus between the  
17 substrate and TiN coatings can cause poor adhesion, which further exacerbates poor tribological  
18 behaviour. The poor tribological performance can be overcome through the application of multi-layer  
19 coatings (MLCs) <sup>13, 18-23</sup>.

20 Diamond-like-carbon (DLC) coatings are widely used for their outstanding tribological properties, such  
21 as low wear and friction combined with biocompatibility <sup>24</sup>. DLC coatings have been considered for  
22 joint implants due to being chemically inert and having a hard wear-resistant surface, however, the low  
23 adhesion of DLC coatings to metallic substrates combined with the high internal residual stresses  
24 complicates their use in critical applications such as biomedical implants. Modern deposition methods  
25 such as HiPIMs have helped to improve the adhesion and durability of these coatings. Studies have  
26 shown that pre-nitride treatment of the SS 316L substrate can improve the adhesion properties of the  
27 subsequently deposited coatings <sup>25-29</sup>. Other studies <sup>30</sup> have shown the use of intermetallic interlayers  
28 between substrate and the DLC coating helped to provide good bonds and improve adhesion. The use  
29 of a TiN interlayer has been shown to improve the mechanical and tribological properties of  
30 conventional DLC coatings.

31 This study carries out the sub-surface modification of SS 316L substrates by plasma nitriding before  
32 the deposition of a variant TiN/DLC MLC. An electro-dynamic shaker fretting tester was used to assess  
33 the fretting performance of the variant coating systems in dry conditions. The aim of this study is to  
34 assess these novel coatings capability to improve the fretting durability of SS 316L femoral stems  
35 against ceramic femoral heads for total hip replacements in-terms of friction and wear.

## 36 2. Materials and Methods

37 This study utilised biomedical grade austenitic stainless steel AISI 316L as the substrate for the duplex  
38 coatings due to its use as a biocompatible material for hip implants. The chemical composition of SS  
39 316L is highlighted in Table 1. The SS 316L samples (20 × 20 × 0.9 mm) were polished to a mirror  
40 finish using varying grades of silicon carbide polishing paper and diamond paste. Sequentially finer grit  
41 sizes (120, 400, 600, 800 and 1200) were used to remove any machining surface marks, followed by  
42 polycrystalline diamond suspension paste.

43 **Table 1. Chemical composition of austenitic SS 316L (wt%).**

C	Cr	Ni	Mo	Mn	P	S	Si	Fe
0.03	16.9	10.72	2.25	1.32	0.022	0.02	0.48	68.27

## 2.1. Substrate Pre-treatment Variants

Pre-preparation of the samples included the SS 316L specimens being cleaned in an ultrasonic bath with ethanol for 15 minutes. All treatments and coatings were carried out in a Hauzer FlexiCoat 850 deposition system and utilised magnetron sputtering. The samples were fixed to a coating substrate table in the vacuum chamber with two-fold rotation. As part of the treatment process some samples were plasma-assisted vacuum nitrided. This involved initially pumping down the chamber to a based pressure of  $9 \times 10^{-6}$  mbar and then heating it up to 485°C for two hours. Plasma surface etching was used to further clean the samples for 45 minutes at a 200 V bias, 60A anode current and 50 sccm argon gas plasma. Plasma nitriding was then conducted between 490-500°C for 120 minutes at a 120 V bias, 50 V bias plasma voltage and 70 sccm gas flow rates for nitrogen. Following this step, the chamber was cooled down to 200°C. After the nitriding treatment some of these samples were gently polished using 400 grit polishing paper. Table 2 provides an overview the variant treatments applied to the substrate before the coatings were deposited.

**Table 2. Summary of treatment variants applied to the SS 316L substrate.**

Variant	Nitrided	Polished (nitride layer)	
Un-nitrided + Unpolished			16
Nitrided + Unpolished	✓		
Nitrided + Polished	✓	✓	17

## 2.2. Deposited PVD Coatings

Three coating variants were deposited on the three variants of pre-treated SS 316L substrates by means of plasma Vapour Deposition (PVD) in a Hauzer FlexiCoat 850 deposition system. The coatings will be referred by the following designations as highlighted in Table 3:

**Table 3. Breakdown of coating variants used in each coating system.**

Sample	Duplex Coating System	
Coating A	TiN	23
Coating B	TiN + Hydrogenated DLC	24
Coating C	TiN + Hydrogen-Free DLC	25

To summarise the following deposition steps were used to produce the coatings:

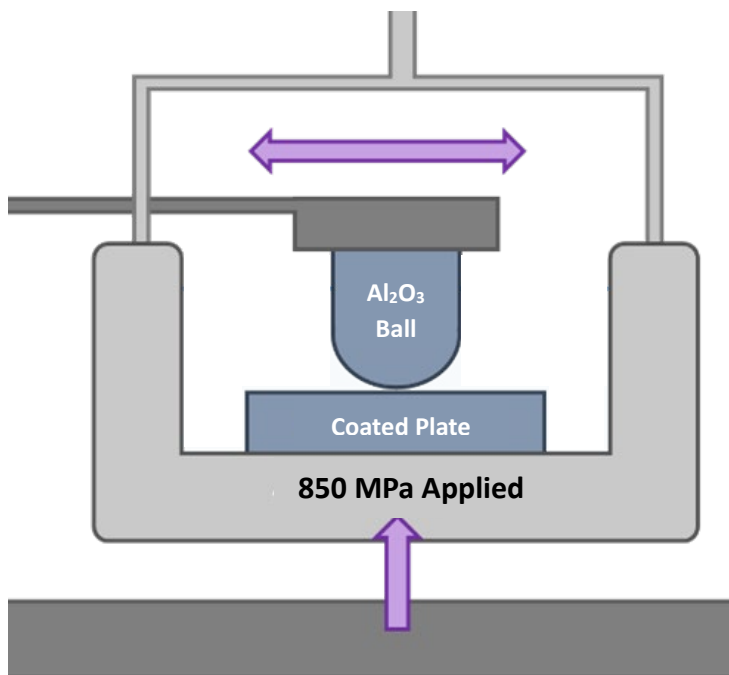
- i) Chamber heating
- ii) Target cleaning
- iii) TiN coating deposition (final step for Coating A)
- iv) H-DLC/H-free DLC coating deposition (for Coatings B and C respectively)

All samples were then prepped for the deposition of a TiN coating using a magnetron sputtering deposition method. The deposition process lasted 90 minutes at 400°C with a 100V bias at 0.3 Pa and 5 kW DC power. The first DLC coating variant was hydrogenated DLC variant and was deposited using a plasma-enhanced chemical vapour deposition method. This used pure C<sub>2</sub> H<sub>2</sub> and Acetylene gas at a 270 sccm flow rate and deposited for 120 minutes at 200°C and 0.8 Pa with a bias voltage of 740V. The second DLC coating variant was a hydrogen-free DLC coating, and this was deposited using a magnetron sputtering deposition method. This used pure Ar gas at 130 sccm flow rate and deposited for 180 minutes at 150°C and 0.3 Pa with a bias voltage of 70V. Both the plasma nitriding and the DLC coating deposition processes were previously developed at the University of Leeds. Surface treatment optimization was not the scope of this paper, hence standard coating recipes were chosen in this study<sup>31</sup>.

## 2.3. Test Methodology

1 A bespoke in-house fretting tribometer with a bespoke electrodynamic shaker utilising a ball-on-plate  
2 configuration was utilised for these experiments. The fretting rig was custom made at the School of  
3 Mechanical Engineering, University of Leeds, UK. Details of the fretting instrument can be found in <sup>32</sup>  
4 and Figure 1 shows a schematic of the setup. The fretting rig applies oscillatory tangential displacements  
5 through an electrodynamic shaker. Normal load (W) was applied through a cantilever system through  
6 the contact interface. Fretting output data includes tangential load (Q) and tangential displacement ( $\delta$ )  
7 which are measured using an axially mounted load cell and optical displacement sensor respectively.  
8 The device was controlled, and data recorded by means of a custom LabVIEW (National Instruments,  
9 USA) programme.

10 Coefficient of friction was calculated using  $\mu = F/N$ , where F is the frictional force (or tangential force)  
11 and N is the normal force. However, the frictional force used was calculated by determining the  
12 frictional force at the maximum velocities in forward and reverse directions, then the average of the  
13 frictional forces of the forward and reverse was calculated.



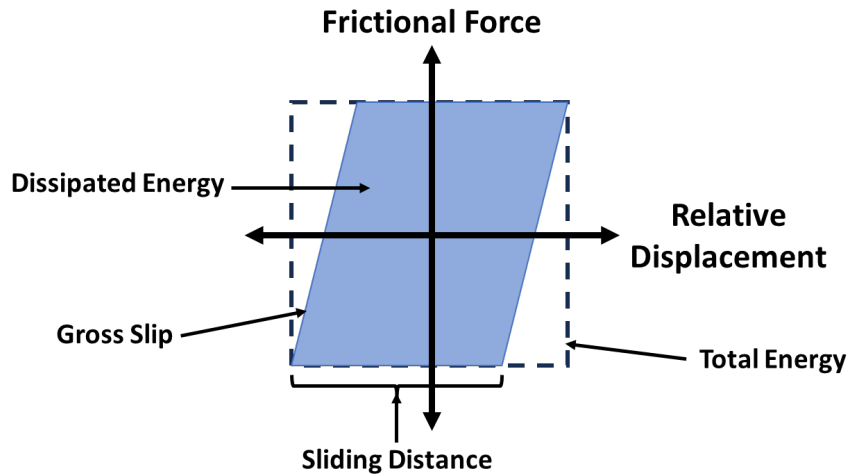
14  
15 **Figure 1. Schematic of bespoke electrodynamic shaker fretting tribometer with ball on plate set-up.**

16 Fretting was replicated by applying micro-motion to the Ø12 Al<sub>2</sub>O<sub>3</sub> ball relative to the duplex coated  
17 SS 316L plate under a dead weight normal load. The applied cyclic displacement and resultant  
18 tangential forces were captured at 400 Hz and analysed as per the frameworks presented by Fouvry et  
19 al <sup>33, 34</sup>. A minimum of three repeats were carried out for each test.

20 A maximum Hertzian contact pressure of 800 MPa was used for the fretting tests, at a fretting  
21 displacement amplitude of 100  $\mu$ m giving a gross slip fretting regime (as determined using sliding ratio)  
22 <sup>35</sup>. Each fretting test lasted 60 minutes or 3600 cycles at a frequency of 1 Hz in dry unlubricated  
23 conditions.

24 Other measured parameters include the energy ratio which is the proportion of total energy that was  
25 dissipated. As shown in Figure 2, this is the area within the curve / (max tangential force\* max  
26 displacement). This was measured for each cycle and averaged over time.

27 Dissipated energy calculated in this study is the force against displacement plotted for each measured  
28 cycle, giving a hysteresis loop. The area within this loop is the energy dissipated. This is done for each  
29 cycle and added together to give the total over time.



1

2 **Figure 2. Example fretting loop for gross-slip regimes Total energy is the area of the dashed region.**  
 3 **Dissipated energy for the gross-slip fretting loops are the enclosed light blue areas, respectively. The sliding**  
 4 **distance for the gross-slip regime is highlighted.**

5 **2.4. Vertical Scanning Interferometry (VSI)**

6 The volume loss from the coated plate samples due to the fretting contact of the ball on flat components  
 7 was measured using an NPFLEX (Bruker, USA) white light interferometer. Surfaces were scanned  
 8 using a non-contact scanning interferometry (VSI) method and using the Vision64 software the surface  
 9 roughness and volume loss of the wear scar on the discs were determined.

10 **2.5. Nano-indentation**

11 The mechanical properties of the various duplex coating systems were assessed using a load-controlled  
 12 partial load nanoindentation using a NanoTest Vantage system, meaning the mechanical properties were  
 13 depth sensitive. A Berkovich diamond indenter with a 120 nm tip radius and a semi-apex angle of  $\sim 65.3^\circ$   
 14 was used for these tests. The instrument had a load resolution of 3 nN and a depth resolution of 0.001  
 15 nm along the z-axis. In total 3 indentations were made with each having 15 loading points, with load  
 16 ranging between 5-500 mN, for each sample. A 0.50  $\mu\text{m/s}$  indenter contact velocity was used with 15 s  
 17 and 5 s load and unload times respectively. A 5 s dwell time at the maximum applied load was used to  
 18 ensure no creep occurred. A 60 s dwell period was used for thermal drift correction. By using the Oliver-  
 19 Pharr methodology<sup>36</sup> the hardness (H) and elastic modulus (E) of the different duplex coated samples  
 20 were calculated.

21 **3. Results**

22 **3.1. Coating Structures and Mechanical Properties**

23 The coating thickness was measured using a Calotest with a 25mm diameter ball and a selection were  
 24 validated using SEM. The results are highlighted in Table 4. Coating A (Table 4(a)) had the thickest TiN  
 25 layers ( $\sim 3\text{-}4\mu\text{m}$ ), compared to when further coatings were deposited which seemed to reduce the  
 26 thickness to just over  $2\mu\text{m}$ . The H-free DLC coatings (Coating C - Table 4(c)) were thicker than their  
 27 hydrogenated DLC (Coating B - Table 4(b)) alternatives, ranging from  $2\text{-}3\mu\text{m}$  compared to  $\sim 1\mu\text{m}$   
 28 respectively.

29 The coating systems mechanical properties and surface roughness are also shown in Table 4. The  
 30 coatings surface mechanical properties are determined through the extrapolation of multi-cycle  
 31 nanoindentations (load-partial unload). The hardness readings correspond to the coating due to the  
 32 penetration depth not exceeding 10% of the coating thickness<sup>37</sup>. The Young's modulus (E) is calculated  
 33 from the average of the maximum range, this is to negate the effects of surface contact which would

1 reduce the modulus at the lower contact depths. Coating A variants had the highest surface roughness  
 2 values and Coating B had the lowest. When comparing the two DLC coating variants, Coating B (H-  
 3 DLC) generally had a lower surface roughness than Coating C (H-free DLC).

4 **Table 4. Summary of surface and mechanical properties (Ra, H & E) of the three coatings variants applied**  
 5 **to SS 316L substrate: a) Coating A, b) Coating B & c) Coating C.**

6 **a) Coating A (TiN)**

Substrate Treatment Variant	TiN Thickness (µm)	Roughness - Ra (µm)	Hardness (GPa)	Young's Modulus (GPa)	H/E
Un-nitrided + Unpolished	2.97 ± 0.04	0.039 ± 0.004	12 ± 12	184 ± 62	0.063
Nitrided + Unpolished	3.41 ± 0.07	0.078 ± 0.002	19 ± 4	217 ± 34	0.089
Nitrided + Polished	3.97 ± 0.04	0.066 ± 0.002	23 ± 4	284 ± 27	0.080

7

8 **b) Coating B (TiN/H-DLC)**

Substrate Treatment Variant	TiN Thickness (µm)	DLC Thickness (µm)	Roughness - Ra (µm)	Hardness (GPa)	Young's Modulus (GPa)	H/E
Un-nitrided + Unpolished	2.96 ± 0.09	1.12 ± 0.06	0.034 ± 0.005	7 ± 1	174 ± 21	0.043
Nitrided + Unpolished	1.97 ± 0.1	0.96 ± 0.02	0.044 ± 0.001	15 ± 5	193 ± 22	0.077
Nitrided + Polished	2.43 ± 0.05	1.11 ± 0.08	0.037 ± 0.003	10 ± 2	194 ± 29	0.049

9

10 **c) Coating C (TiN/H-Free DLC)**

Substrate Treatment Variant	TiN Thickness (µm)	DLC Thickness (µm)	Roughness - Ra (µm)	Hardness (GPa)	Young's Modulus (GPa)	H/E
Un-nitrided + Unpolished	1.84 ± 0.02	2.29 ± 0.02	0.018 ± 0	9 ± 5	116 ± 18	0.075
Nitrided + Unpolished	2.21 ± 0.09	3.15 ± 0.01	0.060 ± 0.001	12 ± 3	140 ± 10	0.086
Nitrided + Polished	2.63 ± 0.01	3.02 ± 0.05	0.055 ± 0.005	12 ± 4	138 ± 10	0.083

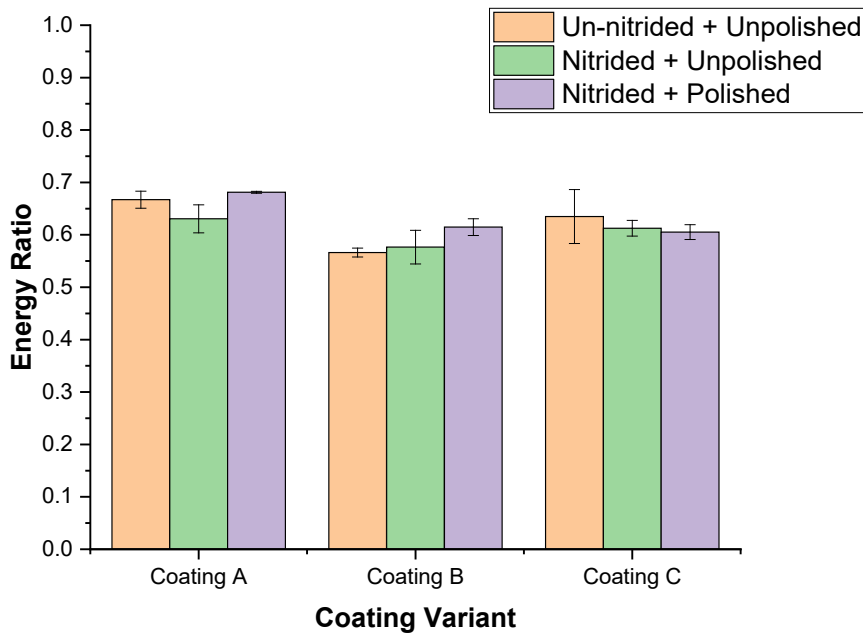
11

12 Coating A variants had the highest surface hardness values and the highest mean elastic modulus  
 13 compared to the other duplex coating systems, with Coating B having the lowest surface hardness and  
 14 elastic modulus. The TiN coating (Coating A) was shown to be harder than DLC coating variants which  
 15 was similar to that observed by Dalibon et al.<sup>38</sup>. When comparing the coating hardness between the two  
 16 DLC coating variants, Coating C (H-Free DLC) generally had a higher hardness than the hydrogenated  
 17 alternative (Coating B) but a lower Young's Modulus. This is most likely due to the different structure  
 18 formations with the different deposition and ion conditions and the presence of hydrogen<sup>39, 40</sup>. A few  
 19 common trends can be observed with the varying treatments for the different coating systems – the un-  
 20 nitrided samples had a lower surface hardness compared to their nitride counterparts and the nitrided +  
 21 unpolished samples generally had a higher hardness trend compared to nitrided + polished samples.

1 Also, the un-nitrided sample variants had the lowest surface roughness whereas the nitrided + polished  
2 samples had the highest.

### 3 3.2. Coefficient of Friction

4 Figure 3 highlights the energy ratio values between measured the dissipated energy and the total energy  
5 during the fretting test. With the energy ratio ranging within 0.2-1 for all tests carried out, indicates all  
6 tests were carried out in gross slip fretting conditions<sup>35</sup>. The instability in the friction data is expected  
7 especially at the beginning stages of the experiment, where the running-in period ranged from 500-2000  
8 seconds depending on the sample variant, until friction reached a steady state value that is maintained  
9 for the remainder of the test. Any significant changes to the coefficient of friction (COF) may give  
10 indications of severe coating/substrate interactions. This can indicate wearing out or the delamination  
11 of the coating<sup>41, 42</sup>.



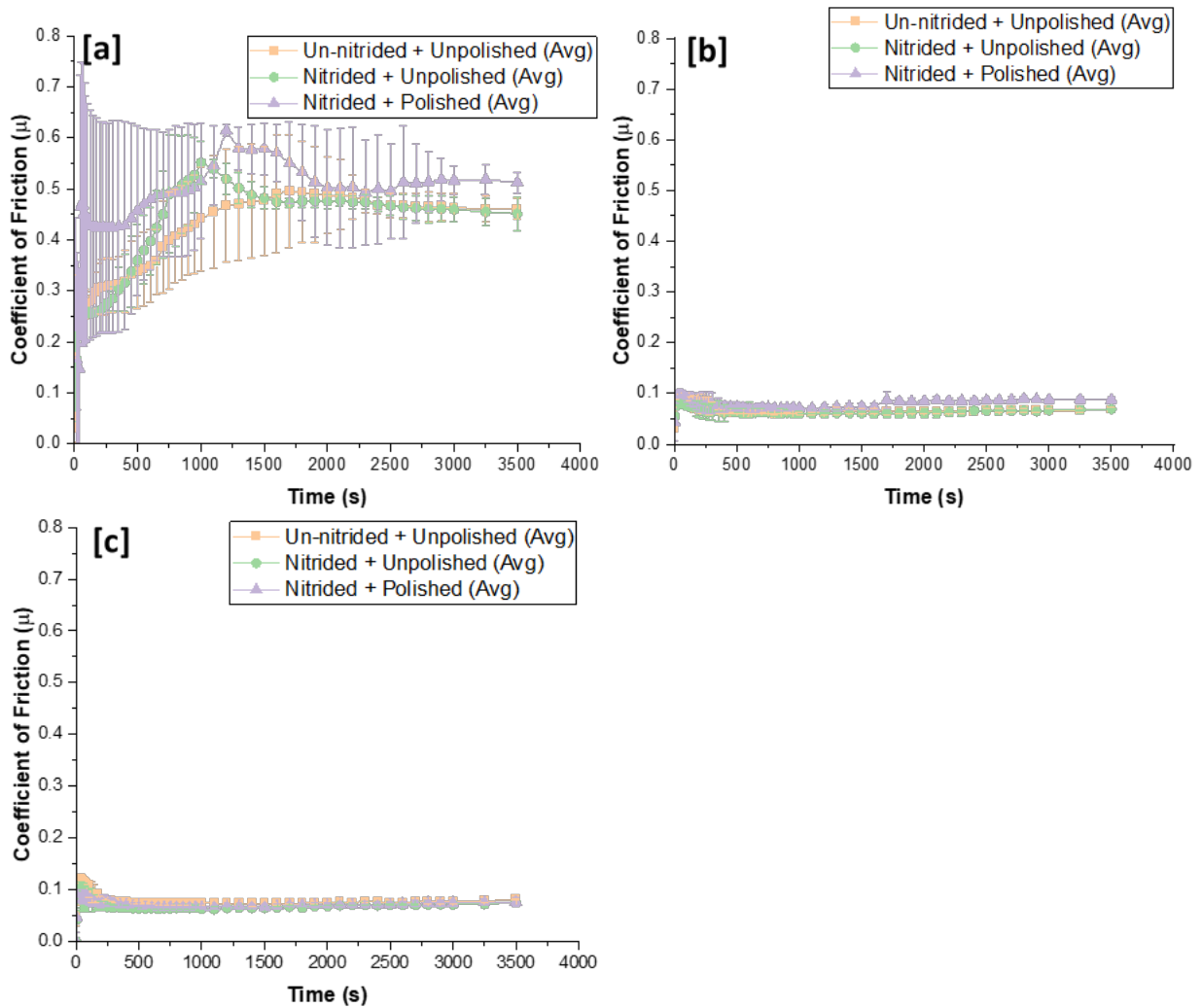
12

13 **Figure 3. Energy ratio of the three coatings variants with varying substrate treatments.**

14 Figure 4 shows the fretting friction results of the three coatings and each of their variants at an applied  
15 pressure of 800 MPa over the entirety of the test. Figure 5 highlights the average COF over the last 30  
16 minutes of testing. The COF was averaged over each cycle (both positive and negative displacement)  
17 and the error bars represent the variability of the friction behaviour between repeated tests at the specific  
18 number of cycles indicated in the figure. This allows for the deviation at each stage of the test to be  
19 analysed and potentially correlated to coating wear. Figure 4(a) highlights the friction behaviour of  
20 Coating A (TiN) variants over the 60-minute duration of the fretting test. With all three variants an  
21 increase in friction behaviour is observed from the beginning of the test until steady state is reached.  
22 However, with Coating B (Figure 4(b)) & C (Figure 4(c)), which were the DLC variants, a different  
23 trend was observed where with the onset of sliding an increase of friction was observed before reducing  
24 and reaching a steady state. With Coating B, after 1750 seconds of testing an increase in friction is  
25 observed before steady state is reached again. With Coating A, the TiN coating variants, a longer  
26 running-in period is observed compared to Coatings B and C. With Coating A, the time to reach steady  
27 state varied between 1500-2000 seconds depending on treatment variation whereas with Coating B and  
28 C this was achieved below 500 seconds. The Coating A variants also demonstrated large variation in  
29 friction behaviour, where the Un-nitrided + Unpolished variant initially reached COF close to 0.4,  
30 whereas the Nitrided + Unpolished and Nitrided + Polished samples reached initial COF's close to 0.5  
31 and 0.6 respectively. This large uncertainty in this coating system was due to variability in the length of

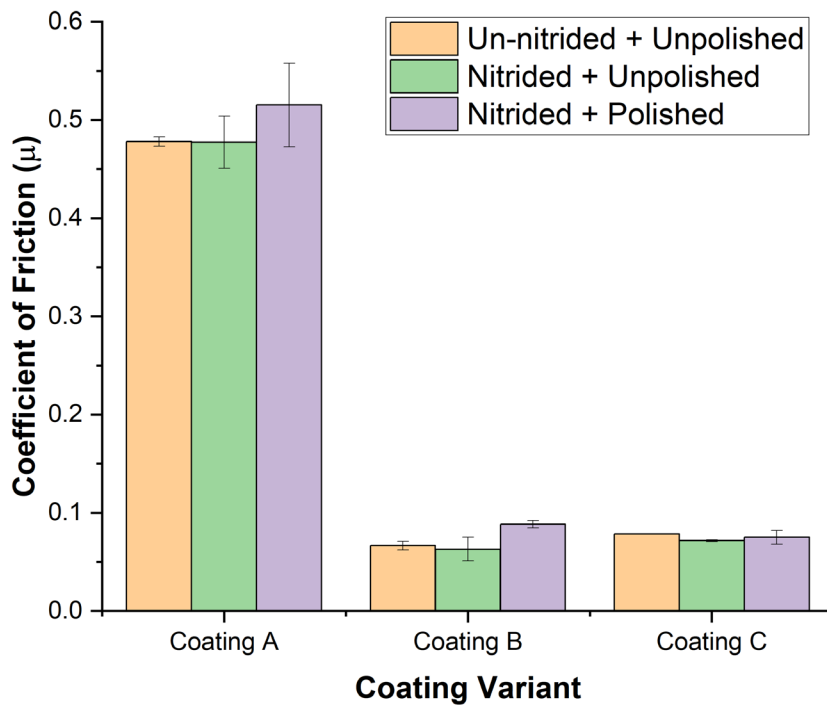


1 time to reach steady state. Overall, Coating A variants demonstrate the highest friction values with  
 2 average COF's close to 0.5, whereas Coatings B & C demonstrate significantly lower trends (<0.1).



3  
 4 **Figure 4. Average coefficient of friction evolution over 3600 secs of three coating system variants with**  
 5 **varying substrate treatment: a) Coating A, b) Coating B & c) Coating C.**

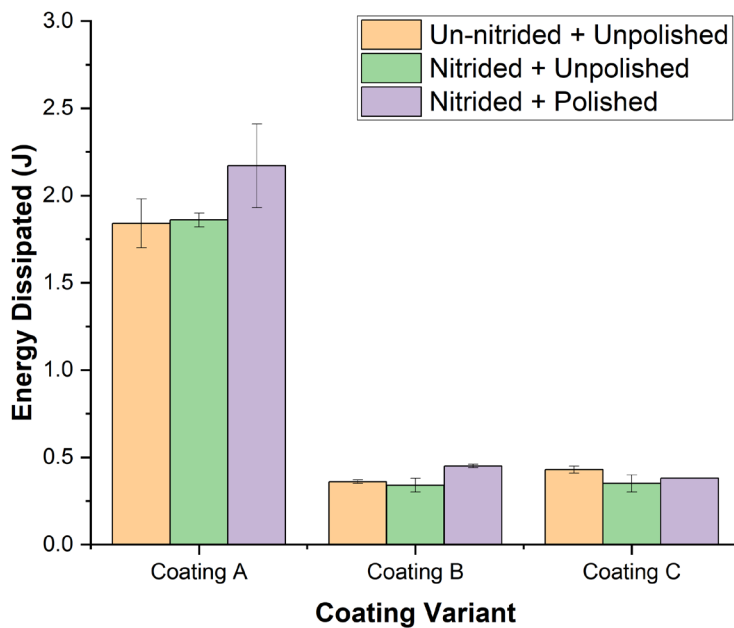
6 From the last 30-minute friction plots (Figure 5) it is possible to see that Coating A (TiN) overall has  
 7 the highest friction trends when steady state is reached (~ 0.5), whereas the steady state friction trends  
 8 from Coatings B (TiN + Hydrogenated DLC) and C (TiN + Hydrogen-free DLC) are significantly lower  
 9 (< 0.1) and very comparable. However overall, all variants of Coating B produced slightly lower friction  
 10 trends in-comparison to Coating C. It was also possible to see from the 60 minute and last 30-minute  
 11 friction plots that the nitrided and unpolished treatment variant for all coatings had the lowest friction  
 12 trends and overall unpolished samples produced lower friction behaviour compared to when they were  
 13 polished.



1

2 **Figure 5. Avg. COF for the last 30 minutes of testing for all three coating variants with varying substrate**  
 3 **treatment.**

4 **3.3. Dissipated Energy**



5

6 **Figure 6. Dissipated energy of the three coatings variants with varying substrate treatments.**

7 The total dissipated fretting energy of each loop can be calculated through integrating the friction force  
 8 and displacement and cumulatively summing the energies. Energy dissipation is a metric that allows  
 9 the wear resistance of each system to be compared<sup>42</sup>. Generally higher dissipated energy correlates with  
 10 increased fretting wear. This quantitative metric can be correlated with wear morphology of each  
 11 fretting scar which would give a complete picture of the system performance.

12 Figure 6 shows the total dissipated energy of all three coating variants. Coating A (TiN) had the highest  
 13 total dissipated energy and Coating B (TiN + Hydrogenated DLC) had the lowest. With all coating

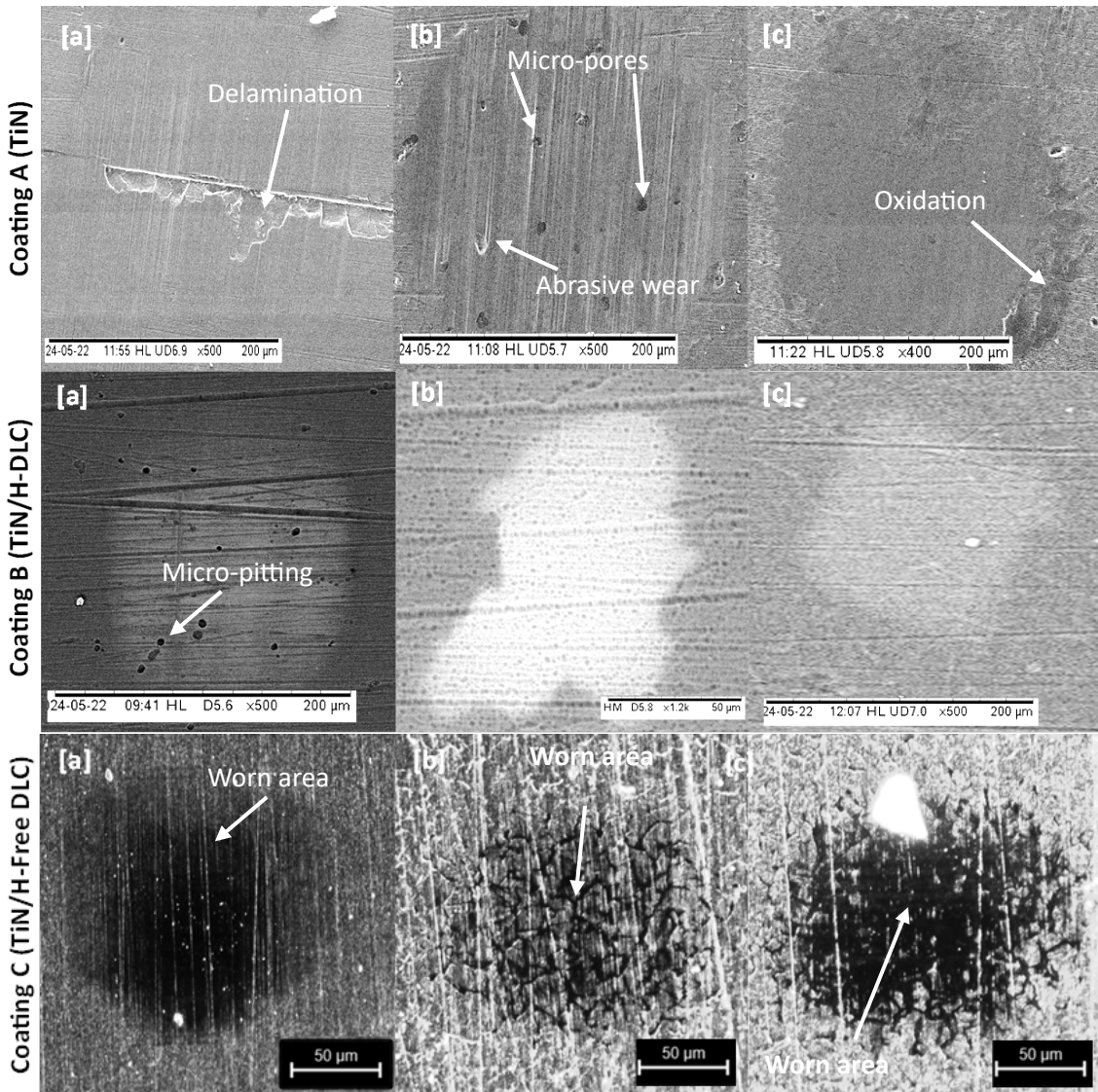
1 variants, the nitrided and unpolished treatment variant gave the lowest total dissipated energy and the  
2 nitrided and polished treatment gave the highest. It can be observed that the unpolished treated samples  
3 had lower wear than when the surface had been polished. The dissipated energy trends (Figure 5) for  
4 the three coating variants generally matched the measured wear trends highlighted in Figure 7.

### 5 **3.4. Wear**

6 SEM (Figure 7) was used to image the fretting scars on the coated plates to qualitatively assess their  
7 morphology. With Coating A (TiN), (a) the un-nitrided + unpolished variant showed coating  
8 delamination and signs of abrasive wear in the wear scar. The coating delamination may have been due  
9 surface imperfections and scratches which would have caused coating discontinuity. With the (b)  
10 nitrided + unpolished variant abrasive wear is observed in the centre of the wear scar alongside micro-  
11 pores. With the (c) nitrided + polished variant of Coating A, oxidative wear is observed around the  
12 edges of the wear scar.

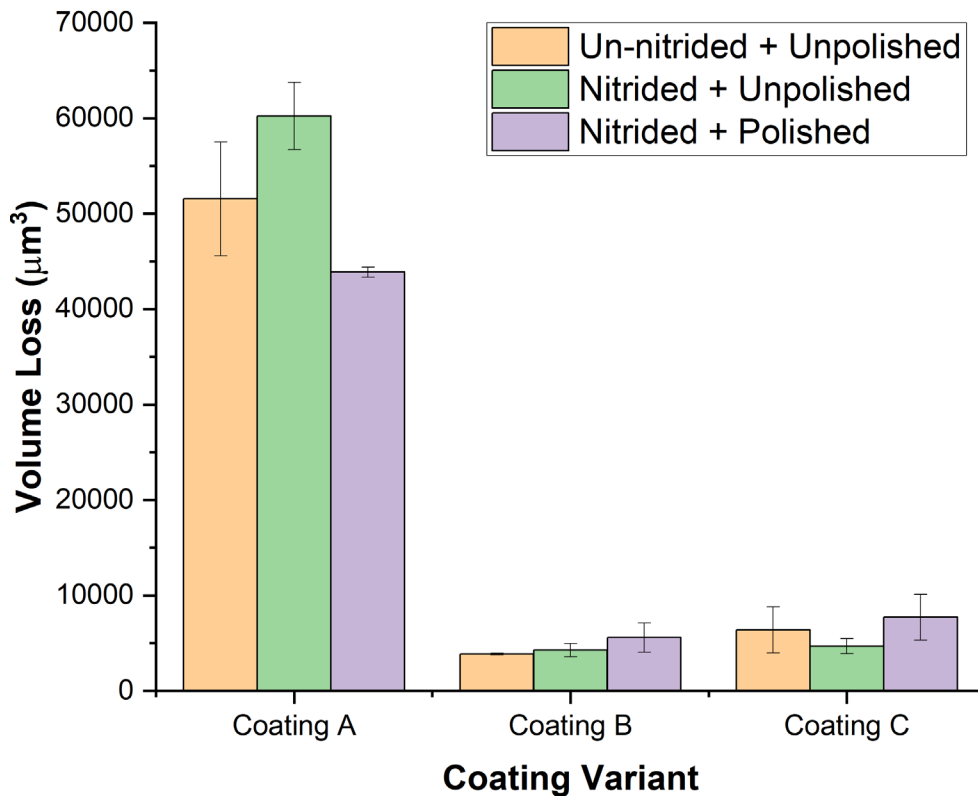
13 With Coating B (TiN/H-DLC), with all substrate pre-treatments the DLC coating appears to be worn  
14 and the wear scar is visible. With (a) the un-nitrided + unpolished variant a more defined wear scar is  
15 observed with micro-pitting present in the wear scar compared to the (b) nitrided + unpolished and (c)  
16 nitrided + polished variant samples.

17 With Coating C (TiN/H-Free DLC), a greater worn surface with micro-pitting can be observed with the  
18 (a) the un-nitrided + unpolished variant compared to the alternative substrate pre-treatments. The  
19 lightest wear scar can be observed with (b) nitrided + unpolished treatment sample.



2  
3  
4

Figure 7. SEM images of the wear scars on the plate samples with the three coating variants with varying substrate pre-treatments: (a) Un-nitrided+Unpolished, (b) Nitrided+Unpolished, (c) Nitrided+Polished.



1

2 **Figure 8. Volume loss from coated plate samples with the three coatings variants with varying substrate**  
 3 **treatments.**

4 Figure 8 compares the wear volume loss from the variant coated plate samples which followed a similar  
 5 trend to the energy dissipated. Coating A (TiN) demonstrated significantly higher volume loss, whereas  
 6 Coating B (TiN + Hydrogenated DLC) had the lowest. The wear volume loss of Coatings B and C were  
 7 very similar, however Coating B demonstrated slightly lower wear. With the DLC coating variants the  
 8 nitrided and unpolished treated samples gave the lowest wear and the nitrided and polished treated  
 9 samples gave the highest. Whereas with Coating A the nitrided and polished treatment variant gave the  
 10 lowest wear and the nitrided and unpolished variant gave the highest.

11 **4. Discussion**

12 In this study, Coating A, a single TiN layer coating, exhibited better mechanical properties than  
 13 alternative multi-layer coatings, however the tribological performance was significantly worse. This  
 14 could be due to hard particles being generated within the contact leading to severe abrasive wear as  
 15 shown in Figure 7a where coating delamination and micropore wearing is observed. The pre-treatment  
 16 of the substrate and the presence of an interlayer coating before the deposition of a variant DLC coating  
 17 (Coatings B & C) significantly improved tribological behaviour. The aim of this study was to assess the  
 18 effects of substrate pre-treatment variance and multi-layer coatings on the fretting performance for bio-  
 19 medical applications.

20 With fretting tests friction measurements are usually deemed a secondary metric with wear being the  
 21 primary focus. With multilayer coatings, under cyclic fatigue conditions wear can cause crack  
 22 nucleation and propagation leading to the formation of wear debris. Friction readings allow for the  
 23 fretting regime to be calculated alongside displacement in relation to the contact area<sup>43</sup>. The hardness  
 24 results show that the nitriding process can increase the hardness of coating system by up to 20% and  
 25 improve load-bearing capacity<sup>44</sup>. Studies have shown that the increase in substrate hardness can  
 26 improve film deposition adhesion or prevent its delamination with the application of a load<sup>45</sup>. The  
 27 introduction of the nitrided layer provides a hardness transition between the softer substrate and harder

1 DLC coating and prevents an eggshell-like effect occurring. Several studies <sup>46-48</sup> have shown that  
2 hydrogen-free DLC coatings have higher hardness and are denser than hydrogenated DLC alternative  
3 coatings, most likely due to higher sp<sup>3</sup> bonding. Furthermore, the surface roughness of the substrate has  
4 a significant effect on the friction and wear behaviour of DLC coatings <sup>44, 49, 50</sup>. The higher surface  
5 roughness of the hydrogen-free DLC (Coating C) compared to the hydrogenated DLC (Table 4) may  
6 account for the slightly higher friction behaviours observed <sup>48</sup>.

7 With all coating variants, with the onset of sliding the increase in friction behaviour could be down to  
8 numerous reasons such as the roughness of the coating, the presence of macroparticles and then the  
9 formation of loose particles separated from the coated surfaces <sup>51</sup>. Coating B & C with the DLC coating  
10 variants had the lowest friction (0.11-0.14) which was similar to other studies where the formation of a  
11 transfer layer with graphitic properties is formed and has a lubricious effect <sup>52, 53</sup>. Graphite has a layer-  
12 by-layer structure, where there is weak van der Waals force between the layers making it easy to shear  
13 hence low friction is observed <sup>54, 55</sup>. Coating A (TiN) presented the highest friction coefficient which  
14 could be due to the higher roughness of the coating (Table 4) which requires higher energy to cause the  
15 plastic deformation of the asperities <sup>56</sup>.

16 The high wear and delamination of the TiN coating (Figure 7) matches that observed in other studies <sup>13</sup>  
17 where it is believed that the micro-cracks, pores and transient grain boundaries cause these coatings to  
18 exhibit poor wear behaviour. Lepicka et al. <sup>57</sup> also observed the high wearing of TiN coatings due to the  
19 peeling off and wear of the coating compared to a DLC coatings. De Oliveira Junior's <sup>58</sup> study found  
20 that TiN particles generated from the wearing of a protective TiN coating, can lead to severe abrasive  
21 particles present in the contact and a significant increase in wear rate similar to that observed in this  
22 study in Figure 7a.

23 Regarding the wear rates, the DLC coating variants (Coating B & C) in this study gave the lowest wear  
24 rates compared to Coating A (TiN) which matched trends observed with other studies <sup>59</sup>. The DLC  
25 coatings are usually produce a smooth surface due to their amorphous character, and in fretting contacts  
26 topography and surface roughness play an important role as much as hardness <sup>59</sup>. The application of  
27 coatings can be used to improve sample integrity against fretting damage <sup>33</sup>. Those that have residual  
28 compressive stresses are deemed useful due to protection against cracking phenomena. Liskiewicz et  
29 al. <sup>60</sup> investigated the durability of various hard coatings under fretting wear and the total dissipated  
30 energy density before the coating system failed. They showed that mechanical properties of coatings  
31 impact component durability, coatings with a high Young's Modulus produced the highest wear. Similar  
32 trends were observed in this study where all variants of Coating A had the highest Young's modulus and  
33 highest wear. The Young's modulus variance between the substrate and coating can negatively affect  
34 wear performance, which may lead to the easier deformation of the substrate and the generation of  
35 particles from brittle cracking. This combined with the coating containing micro-pores and transient  
36 grain boundaries would have contributed to its poor wear properties. Gomez et al. <sup>29</sup> found that the pre-  
37 nitriding of SS 316L samples prior to the deposition of DLC coatings, thus negating the Young's  
38 modulus difference between the substrate and coating, improved coating adherence and increased dry  
39 wear resistance and a low coefficient of friction, matching the trends observed in this study.

40 Several studies have shown that the H/E ratio of the coatings can impact tribological performance. A  
41 high H/E ratio can indicate superior wear resistance which was similar to some of the trends observed  
42 in this study <sup>61, 62</sup>. With each coating variant, the nitrided and unpolished variant had the highest H/E  
43 ratio and the lowest volume loss. However, the nitrided and polished sample variant had the second  
44 highest H/E ratio, but it had the highest volume loss. This high-volume loss maybe due to a weak  
45 adhesion of the coatings to the surface of the polished nitrided substrate, which would cause quicker  
46 coating delamination and wearing. Miletic et al. <sup>63</sup> found that with TiN coatings the adhesion strength  
47 increased with an increase in the substrate surface roughness. This increase in substrate roughness  
48 occurs alongside an increase in contact area between the substrate and coating. This leads to an

1 improvement in the physical and chemical bonding between the two interfaces and this mechanical  
2 interlocking plays a significant role in the coating adhesion. The study also found an increase in the  
3 critical load needed to cause coating detachment/failure caused by the different deformation modes due  
4 to different surface morphologies. Rougher substrate surfaces require higher energy for the plastic  
5 deformation of surface asperities; therefore, a higher normal load is required to cause coating failure.  
6 Studies<sup>64,65</sup> have found that during the deposition of the TiN coating using an Ar ion beam leads to the  
7 induction of energy into the growing film to enhance the mobility of surface atoms. With substrates  
8 with a rough finish, this treatment results in the averaging of the height points on the film surface and  
9 the film masks some of the substrate asperities and the coated sample becomes smoother. Jiang et al.<sup>66</sup>  
10 found that DLC coatings deposited on to low roughness substrates had a lower wear rate compared to  
11 samples with higher surface finish. These trends correlate with the behaviours observed in this study  
12 and highlighted in Table 4 & Figure 8.

13 Between the two DLC variants – hydrogenated (Coating B) and hydrogen-free (Coating C) DLC  
14 differences in tribological performances were observed. The hydrogenated DLC coatings produced  
15 lower friction and wear behaviour than the hydrogen-free variant producing similar trends to that  
16 observed by Ronkainen et al.<sup>48</sup>. It is believed that the formation of graphitic carbon plays a role in the  
17 lower friction behaviour observed with hydrogenated DLC coating (Coating B). Lower levels of  
18 graphitisation with the hydrogen-free DLC coatings (Coating C) were detected due to its more stable  
19 structure and higher sp<sup>3</sup> bonding. Hence due to this, more energy is required to shear deform the  
20 structure and transform it into a graphitic structure compared to hydrogenated DLC coatings.

21 Other studies<sup>67,68</sup> have also highlighted the importance of hydrogen in impacting the tribological  
22 performance of DLC coatings, where lower friction can only be achieved with hydrogen-free coatings  
23 with the presence of humidity in the testing atmosphere. The studies demonstrated that under dry  
24 conditions, the hydrogen present within hydrogenated DLC coatings helped them to achieve lower  
25 friction trends through graphitic formation compared to the hydrogen-free alternative coating. As  
26 graphite requires humidity to achieve low friction, the presence of hydrogen within the coating plays a  
27 significant role in achieving this.

28 The application of coatings to improve and protect a surface can also lead to a reduction in friction  
29 behaviour and tangential forces which would therefore reduce dissipated energy over several fretting  
30 cycles<sup>69</sup>. This would help to increase coating durability and reduce wear. Investigating the relationship  
31 between mechanical properties and tribological performance is critical for future duplex coating  
32 optimisation for fretting scenarios.

## 33 **5. Conclusions**

34 The duplex TiN and DLC coating systems demonstrated their ability to improve the fretting durability  
35 of SS 316L material used for femoral stems in total hip replacements. The key conclusions drawn from  
36 the work are:

- 37 • The duplex coated (TiN/DLC) samples demonstrated lower friction and wear compared to just  
38 a TiN coating. This could be due to the better adherence of the multi-layer coating and the  
39 nitriding pre-treatment of the substrate.
- 40 • Un-polished substrates prior to coating deposition led to improved tribological performance  
41 most likely due to improve coating adhesion to the substrate surface.
- 42 • Hydrogenated DLC samples showed lower friction performance compared to hydrogen-free  
43 DLC variants most likely due to higher amounts of graphitisation.

## 44 **Declaration of Competing Interest**

45 The authors declare that they have no known competing financial interests or personal relationships  
46 that could have appeared to influence the work reported in this paper.

## 1 Data Availability

2 Data will be made available on request.

## 3 CRediT Statements

4 Thawhid Khan: Conceptualisation, Methodology, Investigation, Writing - Original Draft. Joshua  
5 Armitage: Conceptualisation, Investigation, Methodology, Writing - Original Draft. Michael Bryant:  
6 Conceptualisation, Resources, Supervision, Writing - Original Draft.

7

8 Conceptualization, TK, TL, YY. and MB.; Methodology, MK, MT, CM, GP and MB.; Software, CM and GP.;  
9 Validation, TK and AD.; Formal Analysis, TK.; Investigation, TK and CM.; Resources, TL, HP and MB.;  
10 Data Curation, CM and GP.; Writing – Original Draft Preparation, TK, MT, GP, AD, TL, MB.; Writing –  
11 Review & Editing, MT, TL, HP, YY and MB.; Visualization, TK.; Supervision, TL, HP, YY and MB.; Project  
12 Administration, TK.; Funding Acquisition, TK, TL, YY and MB.

13

## 14 6. References

- 15 1. De Martino I, Assini JB, Elpers ME, Wright TM and Westrich GH (2015) Corrosion and fretting  
16 of a modular hip system: a retrieval analysis of 60 rejuvenate stems. *The Journal of arthroplasty*  
17 **30(8)**:1470-1475.
- 18 2. Dyrkacz RMR, Brandt J-M, Ojo OA, Turgeon TR and Wyss UP (2013) The Influence of Head Size  
19 on Corrosion and Fretting Behaviour at the Head-Neck Interface of Artificial Hip Joints. *The*  
20 *Journal of arthroplasty* **28(6)**:1036-1040.
- 21 3. Fallahnezhad K, Feyzi M, Ghadirinejad K, Hashemi R and Taylor M (2022) Finite element based  
22 simulation of tribocorrosion at the head-neck junction of hip implants. *Tribology international*  
23 **165**:107284.
- 24 4. Fallahnezhad K, Oskouei RH, Badnava H and Taylor M (2019) The Influence of Assembly Force  
25 on the Material Loss at the Metallic Head-Neck Junction of Hip Implants Subjected to Cyclic  
26 Fretting Wear. *Metals* **9(4)**:422.
- 27 5. Lombardo DJ, Siljander MP, Gehrke CK, Moore DD, Karadsheh MS and Baker EA (2019) Fretting  
28 and Corrosion Damage of Retrieved Dual-Mobility Total Hip Arthroplasty Systems. *The Journal*  
29 *of arthroplasty* **34(6)**:1273-1278.
- 30 6. Mroczkowski ML, Hertzler JS, Humphrey SM, Johnson T and Blanchard CR (2006) Effect of  
31 impact assembly on the fretting corrosion of modular hip tapers. *Journal of Orthopaedic*  
32 *Research* **24(2)**:271-279.
- 33 7. Royhman D, Pourzal R, Hall D, Lundberg HJ, Wimmer MA, Jacobs J, Hallab NJ and Mathew MT  
34 (2021) Fretting-corrosion in hip taper modular junctions: The influence of topography and pH  
35 levels – An in-vitro study. *Journal of the Mechanical Behavior of Biomedical Materials*  
36 **118**:104443.
- 37 8. Siljander MP, Gehrke CK, Wheeler SD, Sobh AH, Moore DD, Flierl MA and Baker EA (2019) Does  
38 Taper Design Affect Taper Fretting Corrosion in Ceramic-on-Polyethylene Total Hip  
39 Arthroplasty? A Retrieval Analysis. *The Journal of arthroplasty* **34(7, Supplement)**:S366-  
40 S372.e2.
- 41 9. Ghadirinejad K, Day CW, Milimonfared R, Taylor M, Solomon LB and Hashemi R (2023) Fretting  
42 Wear and Corrosion-Related Risk Factors in Total Hip Replacement: A Literature Review on  
43 Implant Retrieval Studies and National Joint Replacement Registry Reports. *Prosthesis*  
44 **5(3)**:774-791.



- 1 10. Ma L, Wiame F, Maurice V and Marcus P (2019) Origin of nanoscale heterogeneity in the  
2 surface oxide film protecting stainless steel against corrosion. *Npj Materials Degradation*  
3 **3(1)**:29.
- 4 11. Marcolongo M, Sarkar S and Ganesh N (2017) 7.11 trends in materials for spine surgery.
- 5 12. Cook SD, Barrack RL, Baffes GC, Clemow AJ, Serekian P, Dong N and Kester MA (1994) Wear  
6 and corrosion of modular interfaces in total hip replacements. *Clinical Orthopaedics and*  
7 *Related Research*® **298**:80-88.
- 8 13. Amirtharaj Mosas KK, Chandrasekar AR, Dasan A, Pakseresht A and Galusek D (2022) Recent  
9 Advancements in Materials and Coatings for Biomedical Implants. *Gels* **8(5)**.
- 10 14. Sikder P, Ren Y and Bhaduri SB (2019) Synthesis and evaluation of protective poly(lactic acid)  
11 and fluorine-doped hydroxyapatite-based composite coatings on AZ31 magnesium alloy.  
12 *Journal of Materials Research* **34(22)**:3766-3776.
- 13 15. Metroke TL, Parkhill RL and Knobbe ET (2001) Passivation of metal alloys using sol-gel-derived  
14 materials — a review. *Progress in Organic Coatings* **41(4)**:233-238.
- 15 16. Bekmurzayeva A, Duncanson WJ, Azevedo HS and Kanayeva D (2018) Surface modification of  
16 stainless steel for biomedical applications: Revisiting a century-old material. *Materials Science*  
17 *and Engineering: C* **93**:1073-1089.
- 18 17. Safin Kaosar Saad K, Saba T and Bin Rashid A (2024) Application of PVD coatings in medical  
19 implantology for enhanced performance, biocompatibility, and quality of life. *Heliyon*  
20 **10(16)**:e35541.
- 21 18. Chen C-Z, Li Q, Leng Y-X, Chen JY, Zhang P-C, Bai B and Huang N (2010) Improved hardness and  
22 corrosion resistance of iron by Ti/TiN multilayer coating and plasma nitriding duplex  
23 treatment. *Surface and Coatings Technology* **204(18)**:3082-3086.
- 24 19. Samanta A, Rane R, Kundu B, Kr. Chanda D, Ghosh J, Bysakh S, Jhala G, Joseph A, Mukherjee S,  
25 Das M and Mukhopadhyay AK (2020) Bio-tribological response of duplex surface engineered  
26 SS316L for hip-implant application. *Applied Surface Science* **507**:145009.
- 27 20. Yang W, Ayoub G, Salehinia I, Mansoor B and Zbib H (2017) Deformation mechanisms in Ti/TiN  
28 multilayer under compressive loading. *Acta Materialia* **122**:99-108.
- 29 21. Łępicka M, Grądzka-Dahlke M, Pieniak D, Pasierbiewicz K, Kryńska K and Niewczas A (2019)  
30 Tribological performance of titanium nitride coatings: A comparative study on TiN-coated  
31 stainless steel and titanium alloy. *Wear* **422-423**:68-80.
- 32 22. Huang X, Etsion I and Shao T (2015) Effects of elastic modulus mismatch between coating and  
33 substrate on the friction and wear properties of TiN and TiAlN coating systems. *Wear* **338-**  
34 **339**:54-61.
- 35 23. Subramanian B, Ananthakumar R and Jayachandran M (2011) Structural and tribological  
36 properties of DC reactive magnetron sputtered titanium/titanium nitride (Ti/TiN) multilayered  
37 coatings. *Surface and Coatings Technology* **205(11)**:3485-3492.
- 38 24. Kumar A and Singh G (2024) Surface modification of Ti6Al4V alloy via advanced coatings:  
39 Mechanical, tribological, corrosion, wetting, and biocompatibility studies. *Journal of Alloys and*  
40 *Compounds* **989**:174418.
- 41 25. Aisenberg S and Chabot R (1971) Ion-beam deposition of thin films of diamondlike carbon.  
42 *Journal of Applied Physics* **42(7)**:2953-2958.
- 43 26. García J, Díaz C, Mändl S, Lutz J, Martínez R and Rodríguez R (2010) Tribological improvements  
44 of plasma immersion implanted CoCr alloys. *Surface and Coatings Technology* **204(18-**  
45 **19)**:2928-2932.
- 46 27. Gómez I, Claver A, Santiago JA, Fernandez I, Palacio JF, Diaz C, Mändl S and Garcia JA (2021)  
47 Improved Adhesion of the DLC Coating Using HiPIMS with Positive Pulses and Plasma  
48 Immersion Pretreatment. *Coatings* **11(9)**:1070.
- 49 28. Kuang X, Li L, Wang L, Li G, Huang K and Xu Y (2019) The effect of N+ ion-implantation on the  
50 corrosion resistance of HiPIMS-TiN coatings sealed by ALD-layers. *Surface and Coatings*  
51 *Technology* **374**:72-82.

- 1 29. Gómez I, García JA, Santiago JA, Fernandez I, Jose Fernandez P and Braceras I (2022) Adhesion  
2 Enhancement on a Duplex DLC HiPIMS Positive Pulse Coating Performed by Active Screen  
3 Plasma Nitriding Pretreatment on 316L Stainless Steel Substrate. *Advances in Materials  
4 Science and Engineering* **2022**.
- 5 30. Cicek H (2018) Wear behaviors of TiN/TiCN/DLC composite coatings in different environments.  
6 *Ceramics International* **44(5)**:4853-4858.
- 7 31. McMaster SJ, Liskiewicz TW, Neville A and Beake BD (2020) Probing fatigue resistance in multi-  
8 layer DLC coatings by micro- and nano-impact: Correlation to erosion tests. *Surface and  
9 Coatings Technology* **402**:126319.
- 10 32. Oladokun A, Pettersson M, Bryant M, Engqvist H, Persson C, Hall R and Neville A (2015) Fretting  
11 of CoCrMo and Ti6Al4V alloys in modular prostheses. *Tribology-Materials, Surfaces &  
12 Interfaces* **9(4)**:165-173.
- 13 33. Fouvry S, Kapsa P and Vincent L (1996) Quantification of fretting damage. *Wear* **200(1)**:186-  
14 205.
- 15 34. Fouvry S, Kapsa P and Vincent L (2000) Description of fretting damage by contact mechanics.  
16 *ZAMM-Journal of Applied Mathematics and Mechanics/Zeitschrift für Angewandte  
17 Mathematik und Mechanik* **80(51)**:41-44.
- 18 35. Fouvry S, Kapsa P and Vincent L (1995) Analysis of sliding behaviour for fretting loadings:  
19 determination of transition criteria. *Wear* **185(1)**:35-46.
- 20 36. Oliver WC and Pharr GM (1992) An improved technique for determining hardness and elastic  
21 modulus using load and displacement sensing indentation experiments. *Journal of Materials  
22 Research* **7(6)**:1564-1583.
- 23 37. Standardization IOF (2002) *Metallic Materials: Instrumented Indentation Test for Hardness and  
24 Materials Parameters. Test Method*. ISO.
- 25 38. Dalibón EL, Pecina JN, Moscatelli MN, Ramírez Ramos MA, Trava-Airoldi VJ and Brühl SP (2019)  
26 Mechanical and corrosion behaviour of DLC and TiN coatings deposited on martensitic  
27 stainless steel. *Journal of Bio-and Tribo-Corrosion* **5**:1-9.
- 28 39. Robertson J (1992) Properties of diamond-like carbon. *Surface and Coatings Technology*  
29 **50(3)**:185-203.
- 30 40. Robertson J (2002) Diamond-like amorphous carbon. *Materials Science and Engineering: R:  
31 Reports* **37(4)**:129-281.
- 32 41. Hintikka J, Mäntylä A, Vaara J, Frondelius T and Lehtovaara A (2019) Stable and unstable  
33 friction in fretting contacts. *Tribology international* **131**:73-82.
- 34 42. Liskiewicz T and Fouvry S (2005) Development of a friction energy capacity approach to predict  
35 the surface coating endurance under complex oscillating sliding conditions. *Tribology  
36 international* **38(1)**:69-79.
- 37 43. Fouvry S, Liskiewicz T, Kapsa P, Hannel S and Sauger E (2003) An energy description of wear  
38 mechanisms and its applications to oscillating sliding contacts. *Wear* **255(1)**:287-298.
- 39 44. Soprano PB, Salvaro DB, Giacomelli RO, Binder C, Klein AN and de Mello JDB (2018) Effect of  
40 soft substrate topography on tribological behavior of multifunctional DLC coatings. *Journal of  
41 the Brazilian Society of Mechanical Sciences and Engineering* **40(8)**:371.
- 42 45. Komarov FF, Konstantinov VM, Kovalchuk AV, Konstantinov SV and Tkachenko HA (2016) The  
43 effect of steel substrate pre-hardening on structural, mechanical, and tribological properties  
44 of magnetron sputtered TiN and TiAlN coatings. *Wear* **352-353**:92-101.
- 45 46. Ronkainen H, Koskinen J, Likonen J, Varjus S and Vihersalo J (1994) Characterization of wear  
46 surfaces in dry sliding of steel and alumina on hydrogenated and hydrogen-free carbon films.  
47 *Diamond and Related Materials* **3(11-12)**:1329-1336.
- 48 47. Ronkainen H, Varjus S and Koskinen J (1992) Tribological properties of diamond-like carbon  
49 films. *Tribologia* **11(3)**:133-141.
- 50 48. Ronkainen H, Varjus S, Koskinen J and Holmberg K (2001) Differentiating the tribological  
51 performance of hydrogenated and hydrogen-free DLC coatings. *Wear* **249(3)**:260-266.

- 1 49. Holmberg K, Laukkanen A, Ronkainen H, Waudby R, Stachowiak G, Wolski M, Podsiadlo P, Gee  
2 M, Nunn J, Gachot C and Li L (2015) Topographical orientation effects on friction and wear in  
3 sliding DLC and steel contacts, part 1: Experimental. *Wear* **330-331**:3-22.
- 4 50. Lan R, Ma Z, Wang C, Lu G, Yuan Y and Shi C (2019) Microstructural and tribological  
5 characterization of DLC coating by in-situ duplex plasma nitriding and arc ion plating. *Diamond  
6 and Related Materials* **98**:107473.
- 7 51. Jasempoor F, Elmkhah H, Imantalab O and Fattah-alhosseini A (2022) Improving the  
8 mechanical, tribological, and electrochemical behavior of AISI 304 stainless steel by applying  
9 CrN single layer and Cr/CrN multilayer coatings. *Wear* **504-505**:204425.
- 10 52. Donnet C and Erdemir A (2007) *Tribology of diamond-like carbon films: fundamentals and  
11 applications*. Springer Science & Business Media.
- 12 53. Grill A (1997) Tribology of diamondlike carbon and related materials: an updated review.  
13 *Surface and Coatings Technology* **94-95**:507-513.
- 14 54. Polcar T, Novák R and Široký P (2006) The tribological characteristics of TiCN coating at elevated  
15 temperatures. *Wear* **260(1)**:40-49.
- 16 55. Akkaya S, Yıldız B and Ürgen M (2016) Orientation dependent tribological behavior of TiN  
17 coatings. *Journal of Physics: Condensed Matter* **28(13)**:134009.
- 18 56. Kakaš D, Terek P, Miletić A, Kovačević L, Vilotić M, Škorić B and Krumes D (2013) Friction and  
19 wear of low temperature deposited TiN coating sliding in dry conditions at various speeds.  
20 *Tehnicki vjesnik - Technical Gazette* **20**:27-33.
- 21 57. Łępicka M, Tsybrii Y, Kiejko D and Golak K (2021) The effect of TiN and DLC anti-wear coatings  
22 on the tribofilm formation and frictional heat phenomena in coated metals vs. WC-Co.  
23 *Materials* **14(12)**:3342.
- 24 58. Junior MDO, Costa H, Junior WS and De Mello J (2019) Effect of iron oxide debris on the  
25 reciprocating sliding wear of tool steels. *Wear* **426**:1065-1075.
- 26 59. Łępicka M, Grądzka-Dahlke M, Pieniak D, Pasierbiewicz K and Niewczas A (2017) Effect of  
27 mechanical properties of substrate and coating on wear performance of TiN- or DLC-coated  
28 316LVM stainless steel. *Wear* **382-383**:62-70.
- 29 60. Liskiewicz T, Fouvry S and Wendler B (2005) Hard coatings durability under fretting wear. In  
30 *Tribology and Interface Engineering Series*. Elsevier, pp. 657-665.
- 31 61. Leyland A and Matthews A (2004) Design criteria for wear-resistant nanostructured and glassy-  
32 metal coatings. *Surface and Coatings Technology* **177-178**:317-324.
- 33 62. Kaczmarek Ł, Kyziół A, Kottfer D, Szymański W, Kleszcz K and Kyziół K (2024) Mechanical  
34 properties and biocompatibility of multilayer systems based on amorphous SiN:H/SiCN:H  
35 layers on Ti6Al7Nb titanium alloy. *Applied Surface Science* **675**:160947.
- 36 63. Miletić A, Terek P, Kovačević L, Vilotić M, Kakaš D, Škorić B and Kukuruzović D (2014) Influence  
37 of substrate roughness on adhesion of TiN coatings. *Journal of the Brazilian Society of  
38 Mechanical Sciences and Engineering* **36(2)**:293-299.
- 39 64. Jun Q, Jianbin L, Shizhu W, Jing W and Wenzhi L (2000) Mechanical and tribological properties  
40 of non-hydrogenated DLC films synthesized by IBAD. *Surface and Coatings Technology* **128-  
41 129**:324-328.
- 42 65. Zheng WT, Hellgren N, Sjöström H and Sundgren JE (1998) Characterization of carbon nitride  
43 thin films deposited by reactive d.c. magnetron sputtering on various substrate materials.  
44 *Surface and Coatings Technology* **100-101**:287-290.
- 45 66. Jiang J and Arnell RD (2000) The effect of substrate surface roughness on the wear of DLC  
46 coatings. *Wear* **239(1)**:1-9.
- 47 67. Erdemir A, Switala M, Wei R and Wilbur P (1991) A tribological investigation of the graphite-  
48 to-diamond-like behavior of amorphous carbon films ion beam deposited on ceramic  
49 substrates. *Surface and Coatings Technology* **50(1)**:17-23.
- 50 68. Donnet C, Belin M, Auge J, Martin J, Grill A and Patel V (1994) Tribochemistry of diamond-like  
51 carbon coatings in various environments. *Surface and Coatings Technology* **68**:626-631.

- 1 69. Ma L, Eom K, Geringer J, Jun T-S and Kim K (2019) Literature review on fretting wear and
- 2 contact mechanics of tribological coatings. *Coatings* **9(8)**:501.
- 3